Gate Input Capacitance Characterization for Power MOSFETs Using Turn-on and Turn-off Switching Waveforms

Yota Nishitani[1], Michiko Inoue[1], Takashi Sato[2], and Michihiro Shintani[3]

[1]Nara Institute of Science and Technology
8916-5 Takayama-cho, Ikoma, 630-0192, Japan
Email: nishitani.yota.nt2@is.naist.jp

[2]Kyoto University
Yoshida-honmachi, Sakyo-ku, Kyoto, 606-8501, Japan
Email: takashi@i.kyoto-u.ac.jp

[3]Kyoto Institute of Technology
Matsugasaki, Sakyo-ku, Kyoto, 606-8585 Japan
Email: shintani@kit.ac.jp

Acknowledgments

This work was supported by JST-OPERA Program Grant Number JPMJOP1841, Japan.

Keywords

≪MOSFET≫, ≪Simulation≫, ≪Capacitors≫, ≪Transient analysis≫

Abstract

We propose a novel method for characterizing the input capacitance of power metal-oxide semiconductor field-effect transistors (MOSFETs). In contrast with the conventional method, our switching-based characterization extracts gate-source and gate-drain capacitances in a single setup, without partial differentiation. Characterization using both turn-on and turn-off switching waveforms improved the simulation accuracy and reduced the switching timing error by a factor of more than 2.5x.

1 Introduction

Improving the conversion efficiency is the primary goal in the design of power converters, and power metal-oxide-semiconductor field-effect transistors (MOSFETs) are the key devices for improving the conversion efficiency. In recent years, the demand for more efficient power converters has been increasing to realize a low-carbon society. Power MOSFETs using wide-bandgap semiconductors such as silicon carbide (SiC) and gallium nitride (GaN) have exhibited potential for dramatically improving the conversion efficiency [1, 2]. SiC and GaN power MOSFETs can operate at higher switching speeds, with lower losses, and at higher temperatures than conventionally used Silicon (Si) MOSFETs. To take full advantage of these characteristics, circuit simulations play a crucial role in the design of power converters [3].

The accuracy of a circuit simulation is highly dependent on the accuracy of the device models, which represent the device characteristics. The device model of power MOSFETs represents the current and capacitance characteristics. In particular, the gate input capacitance characteristic significantly affects the switching waveform in transient analysis; thus, the characterization of the gate input capacitance is particularly crucial. The gate input capacitance is the sum of the capacitances between the gate-source electrodes (C_{gs}) and drain-gate electrodes (C_{dg}). In general, the input capacitance of a power MOSFET is measured using an LCR meter. During the measurement, the LCR meter provides an operating bias voltage and applies a small signal to measure the impedance between each electrode [4, 5]. Hereafter, this method is called small-signal capacitance (SSC) measurement. However, the operating voltage of power MOSFETs changes dynamically during switching. Consequently, the MOSFETs exhibit operating conditions that differ significantly from the fixed voltages in the SSC measurements. In fact, it has been reported that switching waveforms cannot be accurately represented by device models characterized via SSC measurements [6].

To address this issue, an input capacitance characterization using the turn-on switching waveforms of a double-pulse tester circuit has been proposed [7]. In this method, the input capacitance is characterized by the trajectories of the gate-charge and gate-voltage space during switching. The capacitance model developed using this method can accurately reproduce transient waveforms. Partial differentiation was performed to differentiate between C_{gs} and C_{dg}. To numerically differentiate the measured data, multiple measurements were performed while changing the load current of the double-pulse tester. Therefore, in the region where C_{gs} and C_{dg} are charged simultaneously, it is important to select the bias voltage to perform partial differentiation. In addition, the charge-voltage trajectories during turn-on and turn-off operations may not be consistent. Capacitances obtained using only the turn-on waveforms may not accurately reproduce turn-off waveforms.

This study proposes a novel input capacitance measurement method that is based on [7]. The proposed method takes advantage of the fact that C_{gs} can be treated as a constant, regardless of the gate bias voltage. The drain-gate charge Q_{dg} associated with C_{dg} is obtained by subtracting the gate-source charge Q_{gs} from the total gate charge obtained by the gate current measurement. The drain-gate capacitance C_{dg} can be directly calculated using the obtained Q_{dg}, without partial differentiation. Because partial differentiation is eliminated, the input capacitance is characterized by a switching waveform with a single-load current condition. In addition, separate modeling of turn-on and turn-off behaviors becomes possible, enabling more accurate transient analysis.

The remainder of this paper is organized as follows. In Section 2, we review related studies and explain the motivation for this study. Section 3 describes the proposed input capacitance measurement method. In Section 4, the input capacitance of a commercial SiC power MOSFET is measured using the proposed and conventional methods, and the differences in the measurement results are discussed. Then, the effectiveness of the proposed method was verified by performing simulations using a boost converter. Finally, Section 5 concludes the paper.

2 Switching-based capacitance characterization

This section briefly reviews the approach to obtain the switching-based (SB) capacitance [7]. While widely adopted SSC measurements use a predetermined operating condition, the conventional SB method measures the input capacitance under an actual switching operation with varying bias voltages.

The double-pulse tester circuit shown in Fig. 1 was used for the conventional SB method. When the power MOSFET is turned on, the gate charge Q_g is expressed as

$$Q_g = Q_{gs} - Q_{dg}. \tag{1}$$

By measuring the gate current I_g during turn-on operation, Q_g can be calculated as

$$Q_g = \int I_g \mathrm{d}t = \int \frac{V_{in} - V_{gs}}{R_g} \mathrm{d}t, \tag{2}$$

where V_{in} is the output voltage of the pulse generator and V_{gs} is the gate-source voltage. Q_g was calculated by measuring the potential difference in the external gate resistor R_g. In the measurement, a relatively large R_g is chosen to suppress ringing owing to the parasitic capacitance and inductance as well as to

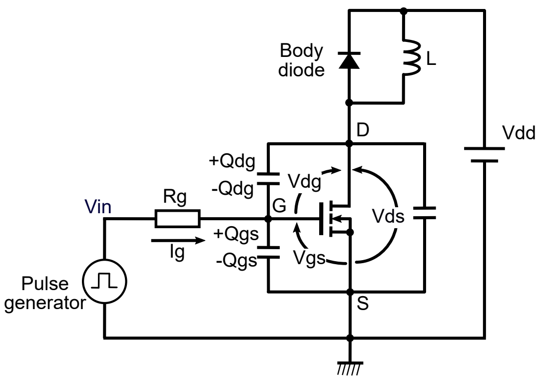

Fig. 1: Double-pulse tester circuit.

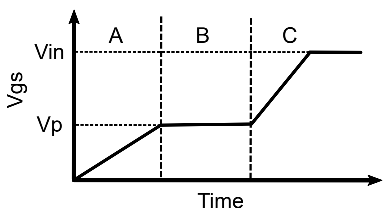

Fig. 2: Gate voltage during turn-on.

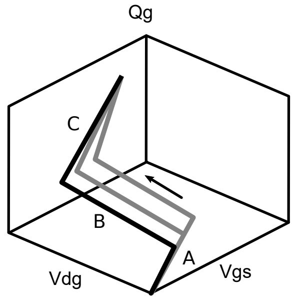

Fig. 3: Turn-on trajectories for different load currents in a $V_{\mathrm{gs}}V_{\mathrm{dg}}Q_{\mathrm{g}}$ space.

reduce the influence of the intrinsic gate resistance of the power MOSFET. By definition,

$$C_{\mathrm{gs}} = \frac{\mathrm{d}Q_{\mathrm{gs}}}{\mathrm{d}V_{\mathrm{gs}}} \tag{3}$$

$$C_{\mathrm{dg}} = \frac{\mathrm{d}Q_{\mathrm{dg}}}{\mathrm{d}V_{\mathrm{dg}}}. \tag{4}$$

Note that Q_{g} is measurable only in this setup. In order to separate Q_{g} into Q_{gs} and Q_{dg}, the authors in [7] made an assumption that "Q_{gs} depends only on V_{gs} and Q_{dg} depends only on V_{dg}." Then, C_{gs} and C_{dg} are derived as the partial differentiations of the gate-source voltage V_{gs} and drain-gate voltage, respectively V_{dg}:

$$\frac{\partial Q_{\mathrm{g}}}{\partial V_{\mathrm{gs}}} = \frac{\partial\left(Q_{\mathrm{gs}} - Q_{\mathrm{dg}}\right)}{\partial V_{\mathrm{gs}}} = \frac{\partial Q_{\mathrm{gs}}}{\partial V_{\mathrm{gs}}} = C_{\mathrm{gs}} \tag{5}$$

$$\frac{\partial Q_{\mathrm{g}}}{\partial V_{\mathrm{dg}}} = \frac{\partial\left(Q_{\mathrm{gs}} - Q_{\mathrm{dg}}\right)}{\partial V_{\mathrm{dg}}} = -\frac{\partial Q_{\mathrm{dg}}}{\partial V_{\mathrm{dg}}} = -C_{\mathrm{dg}}. \tag{6}$$

In this way, C_{gs} and C_{dg} are determined separately.

Here, we consider the gate charge accumulation during the turn-on period. A typical turn-on waveform of V_{gs} is illustrated in Fig. 2. In period "A," C_{gs} is charged primarily until V_{gs} reaches the plateau voltage V_{p}. The period "B" is called the "Miller plateau," where V_{gs} takes a constant value, and only C_{dg} is charged. In period "C," both C_{gs} and C_{dg} are charged until V_{gs} reaches V_{in}.

Fig. 3 shows the trajectories of the switching waveform plotted in a $V_{\mathrm{gs}}V_{\mathrm{dg}}Q_{\mathrm{g}}$ space, where "A," "B," and "C" correspond to the periods shown in Fig. 2. In the double-pulse tester, because the switching waveforms differ depending on the load current, multiple trajectories are drawn, as shown in Fig. 3, collectively forming a plane in the $V_{\mathrm{gs}}V_{\mathrm{dg}}Q_{\mathrm{g}}$ space. The slope along the V_{gs} axis represents C_{gs}, and that

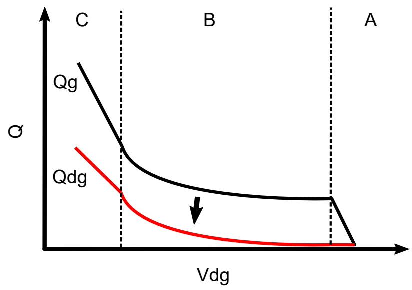

Fig. 4: Gate charge as a function of V_{dg}.

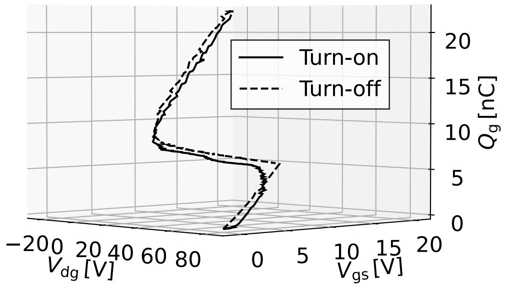

Fig. 5: Switching trajectories during turn-on and turn-off.

along the V_{dg} axis is C_{dg}. These values were obtained by performing measurements with different load currents.

Although the conventional SB method captures capacitances during switching operations more accurately than SSC measurements, the following issues exist:

- Multiple measurements with different load currents are required to form a plane in the $V_{gs}V_{dg}Q_g$ space.
- Determining the bias point to calculate partial differentiation is non-trivial.
- Only turn-on trajectories are used, and turn-on and turn-off characteristics may not match.

3 Switching-based charge-subtraction capacitance characterization

Here, we propose a novel input capacitance characterization method that resolves the aforementioned issues in the SB method. Hereafter, we refer to the proposed method as switching-based, charge-subtraction (SB-CS) capacitance characterization. The SB-CS method uses the same measurement setting as the conventional switching-based, partial differentiation (SB-PD) method. A distinct feature of the SB-CS method is the separation of Q_g to calculate C_{gs} and C_{dg}. We propose to calculate Q_{dg} by subtracting Q_{gs} from Q_g and regarding C_{gs} as invariant. In addition, while the conventional method uses only turn-on waveforms, the SB-CS method uses both turn-on and turn-off waveforms.

The SB-CS capacitance characterization is as follows: First, C_{gs} was calculated from the turn-on trajectory. As explained, charge accumulates mainly in C_{gs} in period "A." Strictly speaking, charge is still transferred to C_{dg} in period "A," but it is sufficiently small compared to C_{gs}. Hence, $Q_g = Q_{gs}$ holds true in this period. Using this period, C_{gs} can be derived as

$$\frac{\mathrm{d}Q_g}{\mathrm{d}V_{gs}} = \frac{\mathrm{d}Q_{gs}}{\mathrm{d}V_{gs}} = C_{gs}. \tag{7}$$

Here, we assume that "C_{gs} is invariant and voltage independent." This is a reasonable assumption because the voltage dependency of C_{gs} is much smaller than that of C_{ds} and C_{dg} in vertical-power MOSFETs [3, 8]. With this assumption, the C_{gs} value obtained using period "A" is used to calculate C_{dg}.

C_{dg} is then calculated as the residual, i.e., Q_{dg} is written as

$$-Q_{dg} = Q_g - Q_{gs} = Q_g - C_{gs} \cdot V_{gs}. \tag{8}$$

Fig. 4 shows the charge trajectory from the V_{dg} direction in the $V_{gs}V_{dg}Q_g$ space. Q_{dg} was obtained by subtracting Q_{gs} from Q_g, and the gradient of the Q_{dg} curve was defined as C_{dg}.

Because the SB-CS method does not rely on partial differentiation, multiple measurements with varying load currents are not required. As we verify later through experiments, the input capacitance can be determined with a single shot under a typical load current condition. Obviously, biased point selection for partial differentiation is no longer necessary.

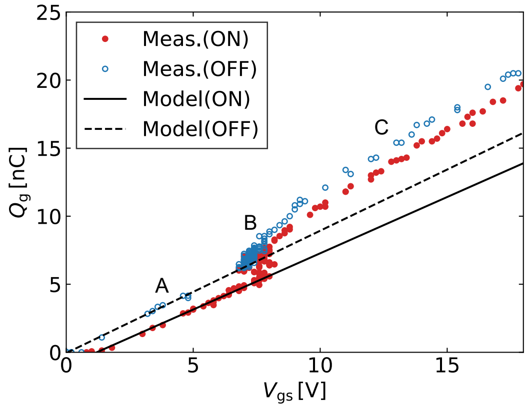

Fig. 6: Measured Q_g-V_{gs} characteristics and its model.

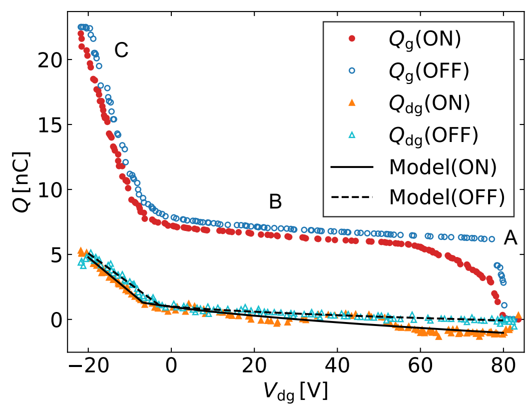

Fig. 7: Q_g-V_{dg} and Q_{dg}-V_{dg} characteristics and Q_{dg} model.

We also propose the use of both the turn-on and turn-off waveforms. Fig. 5 shows the measured waveforms of a commercial SiC power MOSFET (Infineon Technologies AG, IMW120R090M1H, 1200 V, 26 A [9]). The turn-on and turn-off Q_g trajectories are not identical. For such cases, we model the capacitance separately for the turn-on and turn-off transitions. As an example of model implementation, the turn-on capacitance models are written as follows [7]:

$$C_{gs} = \mathbf{CGSO_{on}} \tag{9}$$

$$C_{dg} = \begin{cases} \mathbf{CDGO_{on}} \left(V_{dg} + \mathbf{VJ_{on}}\right)^{-\frac{1}{2}} & (V_{dg} > -0.5\mathbf{VJ_{on}}) \\ \mathbf{COXD_{on}} & (V_{dg} \leq -0.5\mathbf{VJ_{on}}), \end{cases} \tag{10}$$

where the model parameters are in bold. For the turn-off model, the subscript **on** is replaced with **off**. These model parameters can be determined separately from the turn-on and turn-off charge characteristics, respectively. At the point where the C_{dg} function switches, the two functions are implemented to connect smoothly.

4 Measurements and evaluations

The SB-CS method was evaluated using a commercially available SiC power MOSFET (Infineon Technologies AG, IMW120R090M1H, 1200 V, 26 A [9]) as the device under test (DUT). The device models were implemented using Verilog-A [10], and transient analyses were performed using a circuit simulator [11]. For comparison, we applied the SB-PD method [7] to the same DUT.

Capacitance modeling

The double-pulse tester shown in Fig. 1 was used to measure Q_g, where $R_g = 1\,\mathrm{k\Omega}$, $V_{dd} = 80\,\mathrm{V}$, $L = 220\,\mu\mathrm{H}$. A MOSFET body diode of the same type as the DUT was used as the freewheeling diode. $V_{in} = 20\,\mathrm{V}$ was applied using a pulse generator, and the load current was set to 2 A. Fig. 5 shows the measured turn-on and turn-off trajectories. The capacitance characteristics were modeled using Eqs. (9) and (10), and the model parameters were fitted to reproduce these characteristics using simulated annealing [12]. The current characteristics were also modeled to match the drain current measured by the curve tracer using a threshold voltage model [13]. The body diode characteristics were also modeled using the traditional p-n junction diode model [14].

First, to obtain C_{gs}, we used Fig. 6, in which Fig. 5 is viewed from the positive direction of V_{dg}. In Fig. 6, the symbols represent the Q_g-V_{gs} characteristics obtained from the measurement. Closed and open circles indicate turn-on and turn-off, respectively. The solid and broken lines correspond to the fitting results for turn-on and turn-off, respectively. The capacitances of (9) and (10) were integrated and used for fitting as charges. The gate charge Q_g in the period “A” was used for C_{gs} fitting.

Table I: Comparison of model parameters for input capacitance

Parameter	on	off	Conv.
CGSO [pF]	827	899	929
CDGO [pF]	157	78.6	139
COXD [pF]	265	235	381
VJ [V]	13.5	6.05	11.3

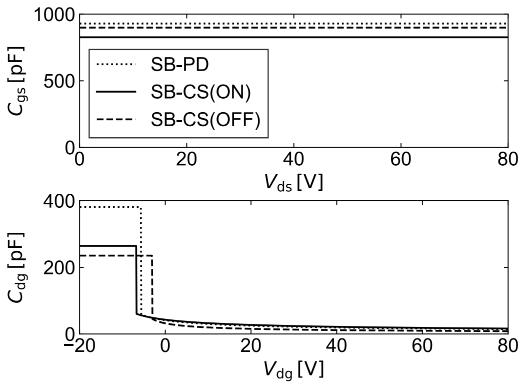

Fig. 8: Comparison of characterized input capacitances.

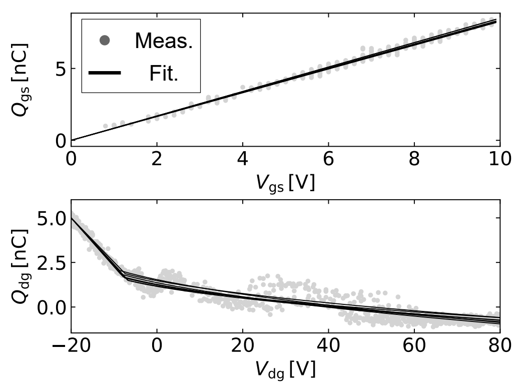

Fig. 9: Load current dependence of charge characteristics.

Fig. 7 shows the measured Q_g-V_{dg} characteristics. The circle and triangle symbols represent Q_g and Q_{dg}, respectively, which were obtained using Eq.(8). The open symbols correspond to the turn-off waveforms. The solid and broken lines represent the fitting results for the turn-on and turn-off waveforms, respectively. It can be observed that the slope of Q_{dg} is significantly reduced when $V_{dg} < 0$ compared to Q_g. Furthermore, those slopes were different for the turn-on and turn-off waveforms, indicating different plateau period lengths.

Comparison of capacitance model parameters

We compared the capacitance models obtained using the SB-CS method with the conventional SB-PD method [7]. For the SB-PD method, the input capacitance was calculated using the turn-on waveform.

Table I lists the model parameters obtained using the SB-CS and SB-PD methods. The capacitance characteristics of C_{gs} and C_{dg}, which were obtained using these parameters, are shown in Fig. 8. C_{gs} obtained by the SB-CS method was almost the same as that obtained by the SB-PD method. However, for C_{dg}, a large difference is observed for $V_{dg} < 0$. This is because of the value of **COXD**; that of the SB-PD method is approximately 1.5 times larger than that of the SB-CS method. In addition, C_{gs} in the region of $V_{dg} < 0$ is approximately three times smaller than C_{dg}. This may be because the slope of C_{dg} could not be determined accurately when taking partial derivatives.

To confirm that the SB-CS method can be used to accurately determine the input capacitance regardless of the load current condition, the change in the charge characteristics was evaluated for various load currents. Fig. 9 shows the measured Q_{gs} and Q_{dg}, as well as the fitting result obtained using the SB-CS method. The load current was varied from 1 A to 7 A in increments of 1 A. The dotted symbols show the measurement of each load current, and the solid lines show the fitting results. The figure shows that the fitting results are almost the same regardless of the load current, indicating that a consistent capacitance characteristic can be obtained at any load .

Transient analysis

To investigate the effectiveness of the capacitance model with a practical circuit, a boost converter was fabricated, and the transient analysis waveforms and measurement results were compared. Transient analyses were performed using two models characterized by the turn-on and turn-off waveforms. The

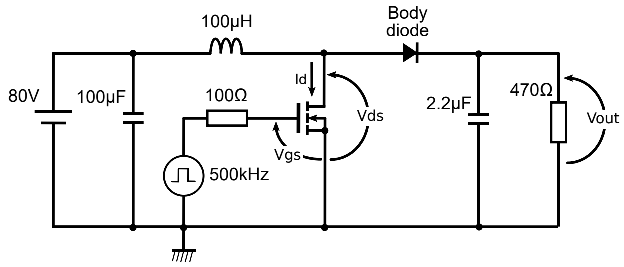

Fig. 10: Circuit diagram of a boost converter.

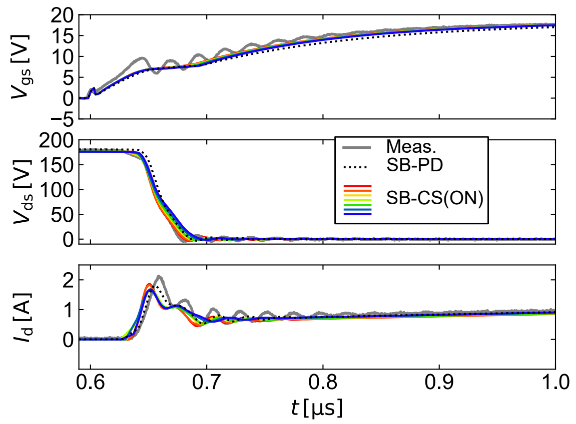

Fig. 11: Simulated and measured turn-on waveforms.

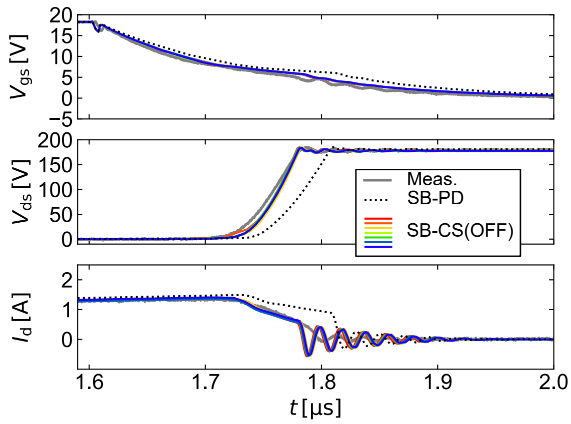

Fig. 12: Simulated and measure turn-off waveforms.

parasitic components of each element, such as the printed circuit board and MOSFET package obtained using an impedance analyzer, were considered in the simulation.

Fig. 10 shows a schematic of the boost converter circuit. The DUT was IMW120R090M1H, and the freewheeling diode was the body diode of the same device as the DUT. A square waveform with an amplitude of 18 V amplitude is applied using a pulse generator. The operating frequency was 500 kHz and the duty ratio was 50%. The measurement and simulation results of the turn-on and turn-off waveforms are shown in Figs. 11 and 12, respectively, where the gray solid line indicates the actual measurement. The colored solid lines and dotted lines are the simulation results obtained using the SB-CS and SB-PD methods, respectively. For the SB-CS method, seven lines are shown in different colors for load currents of 1– 7 A.

In Fig. 11, the V_{gs} waveform of the SB-CS method after the plateau period is in good agreement with the measurements. From the plateau voltage, it can be concluded that the C_{dg} parameter obtained using the SB-CS method is valid. In the SB-PD method, a larger delay of V_{gs} is observed owing to the overestimation of **COXD**. In addition, in the SB-CS method, the simulation results obtained using the capacitance parameters obtained by changing the load current were almost the same. From the transient simulation results, we again confirmed that an arbitrary load current can be used to determine the capacitance parameters.

The SB-CS method reproduced the measured waveform well even for the turn-off waveform, as shown in Fig. 12. In the case of turn-off waveforms, the accuracy of **COXD** affects that of the transient analysis more significantly as the bias condition of the C_{dg}-V_{dg} characteristic transitions from negative to positive values. Therefore, a larger error was observed over the entire switching waveform for the SB-PD method than for the turn-on analysis. Furthermore, from Fig. 12, we can confirm that the load current of the proposed method does not significantly affect the results of the transient analyses.

To evaluate the simulation accuracy quantitatively, we compared the timing errors between the measure-

Table II: Timing error between measured and simulation

	V_{gs}		V_{ds}		I_d	
	SB-PD	SB-CS	SB-PD	SB-CS	SB-PD	SB-CS
Turn-on [ns]	59.8	23.8	2.4	−2.6	−1.4	−5.4
Turn-off [ns]	6.2	2.2	26.4	3.4	34.2	−6.8

ment and simulation at $V_{gs} = 15\,\text{V}$. The timing error in the capacitance model determined from the 2 A load current is presented in Table II. For V_{gs}, the SB-CS method reduced timing error by approximately 2.5 times for the turn-on periods and 2.8 times for the turn-off periods. By reducing the timing error of V_{gs}, the timing errors of V_{ds} and I_d were also improved by 7.8 and 5.0 times for V_{ds} and I_d, respectively, at $V_{ds} = 100\,\text{V}$ and $I_d = 1\,\text{A}$.

5 Conclusion

In this paper, we proposed a novel input capacitance measurement method using switching waveforms. The conventional method uses the turn-on waveforms with different load current conditions and required partial differentiation for separating C_{gs} and C_{dg}. However, in the proposed method, C_{dg} is obtained as the difference between Q_g and Q_{gs} by taking advantage of the fact that C_{gs} is nearly bias voltage independent. In addition, the proposed method requires a single measurement and the selection of bias points for partial differentiation is unnecessary. Furthermore, because the trajectory of Q_g is different between the turn-on and turn-off waveforms, separate modeling of the turn-on and turn-off waveforms was performed to improve the accuracy of the transient analysis. The evaluation using a SiC power MOSFET proved that the proposed method can be used to extract consistent input capacitance. We confirmed that the model obtained using the proposed method accurately simulates the measured waveforms of a boost converter and reduces the timing error of V_{gs} in the transient analysis by 2.5x smaller compared with the conventional method.

References

[1] B. Jayant Baliga, *Fundamentals of Power Semiconductor Devices*. Springer, 2008.

[2] T. Kimoto and J. A. Cooper, *Fundamentals of Silicon Carbide Technology: Growth, Characterization, Devices and Applications*. Wiley, 2014.

[3] M. Shintani, Y. Nakamura, K. Oishi, M. Hiromoto, T. Hikihara, and T. Sato, “Surface-potential-based silicon carbide power MOSFET model for circuit simulation,” *IEEE Transactions on Power Electronics*, vol. 33, no. 12, pp. 10 774–10 783, 2018.

[4] T. Funaki, N. Phankong, T. Kimoto, and T. Hikihara, “Measuring terminal capacitance and its voltage dependency for high-voltage power devices,” *IEEE Transactions on Power Electronics*, vol. 24, no. 6, pp. 1486–1493, 2009.

[5] *B1505A Power Device Analyzer/Curve Tracer*, Keysight Technologies, Inc., 2015.

[6] V. Hoch, J. Petzoldt, A. Schlogl, H. Jacobs, and G. Deboy, “Dynamic characterization of high voltage power MOSFETs for behavior simulation models,” in *Proceedings of IEEE European Conference on Power Electronics and Applications*, 2009, pp. 1–10.

[7] K. Oishi, M. Shintani, M. Hiromoto, and T. Sato, “Input capacitance determination of power MOSFETs from switching trajectories,” in *Proceedings of IEEE International Conference of Microelectronic Test Structures*, 2017, p. 4.4.

[8] N. Phankong, T. Funaki, and T. Hikihara, “A static and dynamic model for a silicon carbide power MOSFET,” in *Proceedings of IEEE European Conference on Power Electronics and Applications*, 2009, pp. 1–10.

[9] *IMW120R090M1H datasheet*, Infineon Technologies AG, 12 2020.

[10] C. C. McAndrew, G. J. Coram, K. K. Gullapalli, J. R. Jones, L. W. Nagel, A. S. Roy, J. Roychowdhury, A. J. Scholten, G. D. J. Smit, X. Wang, and S. Yoshitomi, "Best practices for compact modeling in Verilog-A," *IEEE Journal of the Electron Devices Society*, vol. 3, no. 5, pp. 383–396, 2015.

[11] *HSPICE User Guide: Basic Simulation and Analysis Version P-2019.06*, Synopsys, Inc., 2019.

[12] S. Kirkpatrick, C. D. Gelatt, Jr., and M. P. Vecchi, "Optimization by simulated annealing," *Science*, vol. 220, no. 4598, pp. 671–680, 1983.

[13] T. Sakurai and A. R. Newton, "A simple MOSFET model for circuit analysis," *IEEE Transactions on Electron Devices*, vol. 38, no. 4, pp. 887–894, 1991.

[14] G. Massobrio and P. Antognetti, *Semiconductor Device Modeling with SPICE.* McGraw-Hill, 1993.